

# BSA Adsorption onto Magnetic Polyvinylbutyral Microbeads

DENİZ TANYOLAÇ, AHMET R. ÖZDURAL

Chemical Engineering Department, Hacettepe University, Beytepe 06532, Ankara, Turkey

Received 9 December 1999; accepted 6 April 2000

**ABSTRACT:** Bovine serum albumin (BSA) adsorption onto novel and feasible magnetic polyvinylbutyral-based microbeads was investigated. The microbeads were made of Mowital® B30HH, a commercial product, in the range 125–250  $\mu\text{m}$  by a modified solvent evaporation technique. Magnetite particles were embedded in the polymer structure for favorable magnetic properties, 4.80 emu/g microbeads of saturation magnetization at 6000 Gauss magnetic field. Glutaraldehyde (GA) was used as a bonding agent to increase stability and as a ligand for protein adsorption. The amount of adsorbed BSA was optimized by changing the medium pH and the initial concentrations of GA and BSA. Dynamic adsorption data of batch runs fitted best to Langmuir kinetics. The parameters  $q_{\text{max}}$ ,  $k_f$  and  $k_r$  of the model were estimated through nonlinear regression analysis as 138 mg BSA/g adsorbent, 0.058 ml/(mg BSA  $\cdot$  min) and 0.002  $\text{min}^{-1}$ , respectively, for magnetic microbeads at pH 5.0 and 25°C. The adsorbed BSA was eluted successfully at pH 8.0 and 25°C. Possibly due to surface roughness and magnetic properties,  $q_{\text{max}}$  was found higher than the other adsorbents reported in the literature. The results denote that these microbeads can be an alternative protein adsorbent due to high adsorption capacity and rate, as well as remarkable separation characteristics. © 2001 John Wiley & Sons, Inc. *J Appl Polym Sci* 80: 707–715, 2001

**Key words:** magnetism; protein purification; polyvinylbutyral; bovine serum albumin; adsorption

## INTRODUCTION

Affinity protein separations rely on the highly specific binding between a protein in solution and an immobilized ligand to achieve a high degree of protein purification.<sup>1,2</sup> Methods for synthesizing affinity adsorbents are based on one of two general procedures; either the ligand or ligand analog is reacted with the adsorbent already possessing the spacer arm, or a ligand analog containing the spacer arm is reacted with the activated adsorbent.<sup>3,4</sup> The spacer arm must have reactive ends for attachment to both matrix and ligand. In some cases, the ligand–spacer arm combination is syn-

thesized from smaller components rather than an attempt made to link them in one step.<sup>5,6</sup>

The chemistry of the activation process may involve the reaction of hydroxyl groups on the polymeric matrix, and the most commonly used reaction has been with cyanogen bromide.<sup>3</sup> Although cyanogen bromide activation is still the most widely used method, especially for attachment of proteins through  $\epsilon$ -lysine groups, other convenient and efficient methods are now available, and undoubtedly will substitute the cyanogen bromide procedure eventually. Among these prospective methods; glutaraldehyde, epoxy, carbonyl diimidazole, tosyl chloride, divinylsulphane, monohalogen acetyl halides and epychlorhydrine activations are common.<sup>1,7–9</sup> It is apparent from these methods that the ligand concentration may affect various systems differently,

---

Correspondence to: Deniz Tanyolaç.

*Journal of Applied Polymer Science*, Vol. 80, 707–715 (2001)  
© 2001 John Wiley & Sons, Inc.

and hence, should be considered early in the development of the chromatography process. Very little work has been published to show the effect of ligand concentration on either adsorption equilibrium or adsorption kinetics.<sup>10–13</sup> However, the data such as this will be necessary for reliable modeling and scale-up of these adsorption processes. In a previous study, equilibrium and kinetic parameters were determined for protein adsorption onto two gels containing different amounts of immobilized Cibacron Blue.<sup>14</sup>

Recently, there has been increasing interest in the use of magnetic carriers for separation processes.<sup>15–20</sup> Magnetic carriers can be produced using inorganic materials or a number of synthetic and natural polymers.<sup>21</sup> High mechanical resistance, resistance to solvents, and excellent shelf life make inorganic materials ideal carriers. The main disadvantage of inorganic supports is their limited functional groups for specific binding. Porous or nonporous magnetic carriers are more commonly manufactured from polymers because they have a variety of surface functional groups that can be tailored to use in specific applications.<sup>22</sup>

This article presents the results of a series of experiments in which a model protein, specifically bovine serum albumin (BSA), was adsorbed onto magnetic and nonmagnetic polyvinylbutyral microbeads prepared in spherical and uniform form in the range 125–250  $\mu\text{m}$  from a commercial product, Mowital®, B30HH. Polyvinylbutyral polymer was selected due to its low cost and high concentration of hydroxyl groups on the surface such as agarose, cellulose, or polyacrylamide matrix. Glutaraldehyde (GA) was selected as the agent for surface activation, and the bovine serum albumin was employed as the model protein. The conditions of surface activation; medium pH and initial concentration of GA, were optimized to investigate the adsorption at different equilibrium bovine serum albumin concentrations. The adsorption of BSA in a batch system was elucidated through nonlinear regression analysis to calculate constants of adsorption kinetics from dynamic data. Finally, adsorbed BSA on magnetic and nonmagnetic microbeads was eluted by shifting the medium pH.

## EXPERIMENTAL

### Materials

Mowital® B30HH (polyvinylbutyral, Hoechts, Germany) is the main polymeric matrix for the

**Table I Polymerization Recipe and Experimental Conditions for Magnetic and Nonmagnetic Microbeads**

Component/Condition	Amount
Mowital	20 g
Magnetite <sup>a</sup>	1.5 g
Pluronic PE6800	5 mL (6% v/v)
PVA	4 g
SDS	2 g
Chloroform	100 mL
Distilled water	400 mL
Processing time and temperature	16 h, 20°C
Mixing rate	700 rpm

<sup>a</sup> Not used for nonmagnetic microbeads.

preparation of microbeads. Type B30HH has a better solubility in aromatics than the other forms of Mowital®.<sup>23</sup> The film formation and solubility properties, reactivity of the polymer, and combination capabilities are determined largely by acetalization, hydroxyl group content, and degree of polymerization.

Chloroform (BDH, UK) was used as solvent due to its high capacity for dissolving Mowital® and quick evaporation rate at room temperature.<sup>23</sup> Other ingredients such as SDS (sodium dodecyl sulphate), pluronic PE6800, and PVA (polyvinyl alcohol) were obtained from Sigma (Milwaukee, WI), Basf (Germany) and Merck (Germany) companies, respectively, and used as received. Bovine serum albumin (BSA) (Fraction V, lyophilized), acetate, and saline phosphate buffers for adsorption/desorption experiments were purchased from Sigma and Merck, respectively. Glutaraldehyde (GA) for surface activation was purchased from Merck. Rock magnetite was obtained from Divriği, Turkey. It was crushed in a roll crusher and sieved to maintain the required particle size fractions (<40  $\mu\text{m}$ ).

### Preparation of Polyvinylbutyral Microbeads

Magnetic polyvinylbutyral microbeads were prepared by a modified solvent evaporation method.<sup>9</sup> The polymerization recipe and conditions for the preparation were given in Table I. For magnetic microbeads, 1.5 g of magnetite, determined to be optimum from preliminary runs, employed in the recipe. Nonmagnetic polyvinylbutyral microbeads were prepared following the same recipe without using magnetite. First, the specified amount of polyvinylbutyral was dissolved in chloroform, and

then this solution was transferred immediately into the distilled water containing the prescribed amounts of magnetite and emulsifiers (SDS, PVA, and pluronic PE 6800) in a continuously aerated and agitated water phase. Then the microparticle emulsion was transferred into a glass reactor of 1 liter and agitated with a mechanical stirrer at 700 rpm for 16 h at 20°C. After allowing the solvent to evaporate, magnetite particles were completely encapsulated in polyvinylbutyral microbeads. The produced microbeads were washed with distilled and deionized water three times to remove impurities physically adsorbed onto the surface of the microbeads.

### Microbead Characterization

#### *Analysis of Magnetism*

The presence of magnetite in the polymeric structure was investigated with ESR spectrophotometer (EL 9, Varian). The magnetism degree of the polyvinylbutyral microbeads was measured in a magnetic field by using a vibrating-sample magnetometer (Princeton Applied Research Corporation, USA).

#### *Scanning Electron Microscopy*

To observe the surface topography of the magnetic and nonmagnetic polyvinylbutyral microbeads, scanning electron micrographs of gold-coated samples were taken with an SEM device (Model: Raster Electron Microscopy, Leitz-AMR-1000, Germany).

#### *FTIR Studies*

FTIR spectrum of the magnetic and plain polyvinylbutyral microbeads were obtained by using a FTIR spectrophotometer (FTIR 8110 Series, Shimadzu, Japan). Dry microbeads, 0.1 g, were completely mixed with 0.1 g KBr (IR grade, Merck, Germany), and pressed into a form of tablet and the spectrum was then recorded.

#### *Glutaraldehyde Activation of Microbeads*

Prior to the activation process, the rinsed microbeads were kept in distilled water for about 24 h and washed again on a glass filter with 0.1M HCl solution and then placed in 1 liter of distilled water to remove remaining impurities. Aqueous GA solution (100 mL) with different initial concentrations (0–8% v/v) were prepared and pH of the solution was fixed at 7.4 with 0.1M saline

phosphate buffer. One gram of microbead was then added to this solution while it was magnetically stirred at 30°C, 200 rpm in dark to prevent the polymerization of GA. After 12 h, determined to be sufficient to activate all hydroxyl groups on the entire surface of microporous microbeads from preliminary runs, the microbeads were removed and washed with distilled water several times to remove the excess activation agent and impurities.

### BSA Adsorption/Desorption Studies

BSA was selected as a model protein for adsorption on GA activated magnetic and nonmagnetic polyvinylbutyral microbeads. All adsorption experiments were conducted batchwise for 2 h, which proved to be a sufficient period in any run, at 25°C with a stirring rate of 200 rpm. In a typical adsorption experiment, an appropriate amount of BSA was dissolved in 25 mL of buffer solution of specified pH (buffered with 0.1M sodium acetate–acetic acid solution) and 1 g of microbead was added to start the adsorption reaction. For dynamic data, 0.1 mL of liquid sample was drawn from the reactor at several time intervals for BSA assay and pH check. For equilibrium data, microbeads were removed from the medium by filtration after equilibrium was reached. The BSA adsorbed onto microbeads (adsorption capacity) was determined by measuring the initial and final concentrations of BSA in the medium spectrophotometrically at 280 nm using a calibration curve prepared previously.

#### *The Effect of Initial GA Concentration on Adsorption Capacity*

GA-activated nonmagnetic microbeads at different initial GA concentrations (0–8%, v/v) were used in batch adsorption runs with an initial BSA concentration of 6 mg/mL at pH 7.4 using 0.1M saline phosphate buffer. At equilibrium, BSA adsorption capacity,  $q^*$ , and concentration,  $C^*$ , were determined to find out the optimum initial GA concentration for maximum BSA adsorption.

#### *The Effect of Medium pH on Adsorption Capacity*

Optimum pH of adsorption onto GA-activated nonmagnetic microbeads was determined by varying the medium pH in the range 4–6 using 0.1M sodium acetate–acetic acid buffer. In each run, initial BSA concentration was maintained at 3 mg/mL and equilibrium BSA adsorption capacity

ity,  $q^*$ , and equilibrium BSA concentration,  $C^*$ , were determined. In any run, medium pH was checked at equilibrium for any deviation from initial set value.

### The Effect of BSA Concentration on Adsorption Capacity

For nonmagnetic and magnetic GA-activated microbeads, initial BSA concentration was changed in the range 0.5–5.5 mg/mL at pH 5.0 and BSA adsorption capacity,  $q^*$ , and BSA concentration,  $C^*$ , were determined at equilibrium.

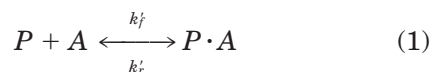
### Desorption of BSA from Microbeads

For the elution of adsorbed BSA, 1 g of magnetic or nonmagnetic microbeads equilibrated at approximately 4 mg/mL BSA, 25°C and pH 5.0 was strained and transferred into 25 mL pH 8.0 ammonia–ammonium chloride buffer solution. The desorption was conducted batchwise at 25°C with a stirring rate of 200 rpm for 1 h. The amount of BSA desorbed from microbeads was calculated by measuring the initial and final concentrations of BSA in the medium.

### Determination of Adsorption Kinetics

GA-activated microbeads present a number of binding sites; thus, protein interactions with the adsorbent are likely to be both heterogeneous and multivalent. A system like this is difficult to model rigorously; therefore, a simplified model of adsorption will be attempted.

The model employed is the second-order reversible reaction, as exemplified in literature for liquid–protein interactions where the protein is assumed to interact with the GA-activated microbeads by a monovalent interaction that has a characteristic binding energy.<sup>10</sup>



where  $P$  is the protein in solution,  $A$  is the GA activated adsorption site and  $P \cdot A$  is the protein-active site complex. The parameters  $k_f'$  and  $k_r'$  are the apparent forward and reverse rate constants, respectively, for the adsorption process. The rate of adsorption for this type of interaction is given by ref. 10

$$\frac{\delta q}{\delta t} = k_f C(q_{\max} - q) - k_r q \quad (2)$$

where  $C$  and  $q$  are the instantaneous solute concentrations in the liquid and on the adsorbent, respectively, and  $q_{\max}$  represents the maximum adsorption capacity of the adsorbent. The rate constants  $k_f'$  and  $k_r'$  are not the intrinsic rate constants for protein interaction with the activated surface of microbeads, but rather are lumped parameters that reflect the contribution of mass transfer resistance relative to the adsorption step. At equilibrium, equations reduce to the familiar Langmuir isotherm model, represented in eq. (3), where  $K$ ,  $C^*$ , and  $q^*$  are the apparent dissociation constant,  $k_r'/k_f'$ , equilibrium solute concentrations in the liquid and on the adsorbent, respectively.

$$q^* = q_{\max} \cdot C^*/(K + C^*) \quad (3)$$

However, at equilibrium, forward and reverse lumped rate constants could not be calculated; thus, the values of  $q_{\max}$ ,  $k_f'$ , and  $k_r'$  were estimated through nonlinear analysis of dynamic experimental data with a nonlinear regression program, Systat<sup>®</sup><sup>24</sup> using eq. (2). In this canned program, coefficients of complex nonlinear models may be evaluated sensitively by nonlinear regression. The required data were taken from the dynamic graph of  $q$  vs.  $t$ , and the term  $\delta q/\delta t$  was calculated numerically.<sup>25</sup> The batch runs were conducted with both GA-activated magnetic and nonmagnetic microbeads at 0.1M sodium acetate–acetic acid-buffered medium pH 5.0, determined to be the optimum pH for adsorption, with an initial BSA concentration of 6 mg/mL.

## RESULTS AND DISCUSSION

### Properties of Polyvinylbutyral Microbeads

Polyvinylbutyral, Mowital<sup>®</sup> B30HH, based microbeads prepared in this study are rather hydrophilic structures. The molecular formula of polyvinylbutyral resin is as follows; it consists of vinylbutyral, vinyl alcohol, and vinyl acetate comonomers in the approximate ratio 75 : 22 : 3, respectively.<sup>23</sup> The polyvinylbutyral microbeads swell rapidly, and the equilibrium is achieved in about 15 min. The equilibrium swelling ratio was about 45% on the weight basis.

The presence of magnetite in the polymeric structure was confirmed by the ESR. A peak of magnetite (i.e., Fe<sub>3</sub>O<sub>4</sub> fine particles) was detected



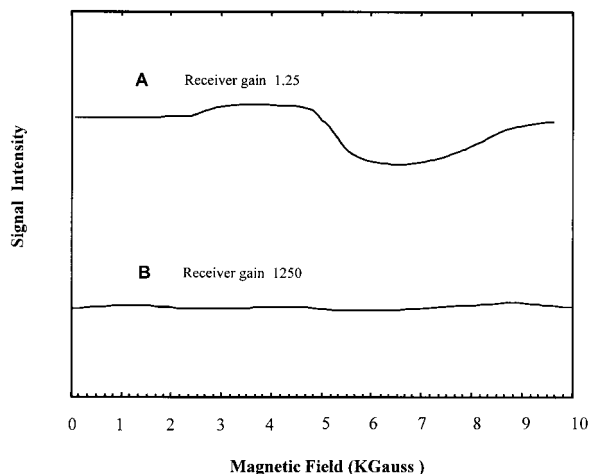


**Figure 1** ESR spectra of (a) magnetic (b) nonmagnetic polyvinylbutyral microbeads.

in the ESR spectrum, as shown in Figure 1. After the glutaraldehyde activation, the intensity of the magnetite peak did not change in ESR spectra of the microbeads. These microbeads were kept in distilled water and ambient air for 6 months, and the same ESR spectra was obtained.

The behavior of magnetic microbeads in a magnetic field using a vibrating magneto-meter was given in Figure 2 in terms of emu, which is related to the intensity of magnetization of the sample vs. applied magnetic field. In this spectra, 6000 Gauss magnetic field with a saturation magnetization 4.80 emu/g microbeads was found sufficient to excite all of the dipole moments of 1.0 g

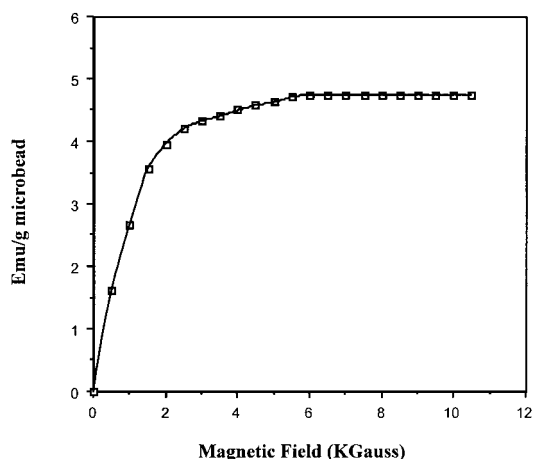


**Figure 2** The magnetic behavior of magnetic polyvinylbutyral microbeads.

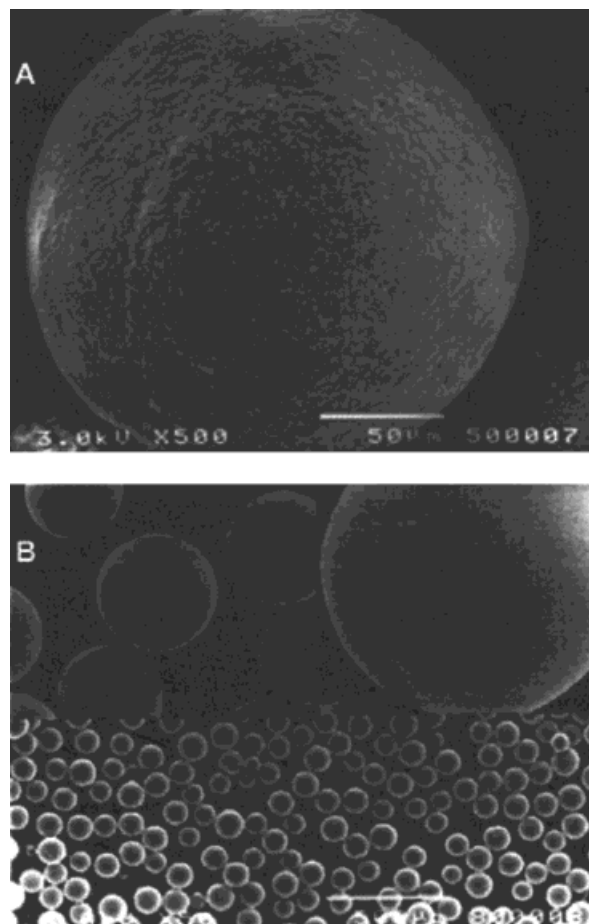


**Figure 3** SEM photographs of (a) magnetic (b) nonmagnetic microbeads.

microbeads containing prescribed amount of magnetite. This magnetic field value will be an important design parameter for a magnetically fluidized bed or for a magnetic filtration using these microbeads. In the literature, this value changes from 8 to 20 kG for various applications with smaller saturation magnetization values than 4.80 emu/g microbeads; thus, prepared magnetic microbeads will need less magnetic intensity in a magnetically fluidized bed or for a magnetic filter.<sup>19,20</sup>

Figure 3 shows the SEM micrographs of magnetic and nonmagnetic polyvinylbutyral microbeads. As clearly seen, the magnetic microbeads have a spherical shape and rough surface with embedded magnetite particles within the structure. These surface properties of the magnetic microbeads would favor better adsorption of the BSA protein due to enhanced

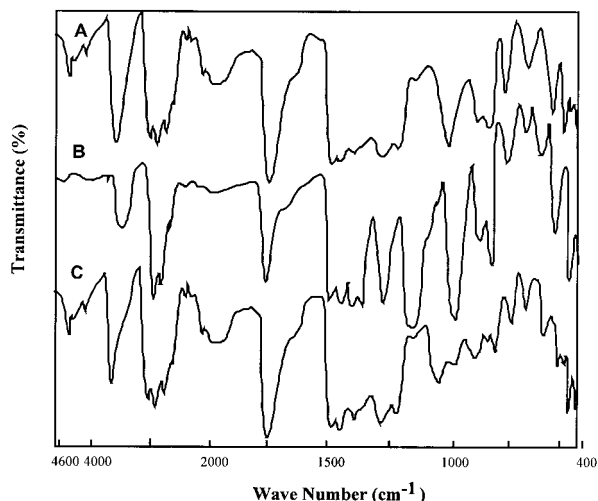


**Figure 4** FTIR spectra of (a) nonmagnetic plain; (b) nonmagnetic GA-activated (c) magnetic microbeads.

surface area and proportionally increased active sites. On the other hand, nonmagnetic microbeads [Fig. 3(b)] were in uniform and spherical shape with smooth surface characteristics.

As mentioned before, GA was selected as the affinity ligand, and attached onto polyvinylbutyral microbeads. Figure 4 gives the FTIR spectra of (a) nonmagnetic (b) GA-activated nonmagnetic, and (c) magnetic polyvinylbutyral microbeads. The presence of hydroxyl functional group on the surface of plain microbeads was confirmed by FTIR spectrophotometer in Figure 4(a). The hydroxyl band observed at  $3500\text{ cm}^{-1}$  indicated the presence of PVAL on the microbead surface. After GA activation, the intensity of the hydroxyl band decreased due to the reaction took place between hydroxyl and aldehyde groups [Fig. 4(b)]. In this spectrum, hydroxyl band peak was decreased, while the  $\text{C}=\text{O}$  band at  $1740\text{ cm}^{-1}$  was increased compare to inactivated microbeads due to reaction of glutaraldehyde with hydroxyl groups to yield the  $\text{C}=\text{O}$  bands. The intensity of  $\text{H}-\text{C}=\text{O}$  and  $\text{CH}_3-\text{C}=\text{O}$  groups increased after GA activation at  $1740\text{ cm}^{-1}$ , respectively. These bands confirmed the reaction of GA with hydroxyl groups on polyvinylbutyral microbeads. The FTIR spectrum of magnetic beads [Fig. 4(c)] showed almost the same characteristics of Figure 4(a), implying unaltered properties of surface chemistry.

## BSA Adsorption/Desorption Studies

### The Effect of Initial GA Concentration on Adsorption Capacity

BSA was adsorbed onto GA-activated nonmagnetic microbeads using different initial GA concentrations, and the results were presented in Figure 5. The runs were repeated three times, and the average values of corresponding data (with a standard deviation not more than 3%) were given in the figure.

The curve indicated that the optimum initial glutaraldehyde concentration for surface activation was around 4% (v/v) with an equilibrium adsorption value of 14 mg BSA/g adsorbent for an initial BSA concentration of 6 mg/mL. Any GA concentration less than 4% (v/v) resulted in insufficient activation of the surface, while higher concentrations caused excessive self-crosslinking of glutaraldehyde, which might have a steric effect for BSA. The maximum BSA adsorption capacity obtained with inactivated particles was 0.45 mg BSA/g adsorbent, which was less than the value 14 mg BSA/g adsorbent obtained with glutaraldehyde activated microbeads. Thus, 4% (v/v) initial glutaraldehyde concentration was applied to the surface activation of the microbeads.

### The Effect of Medium pH on Adsorption Capacity

Prior to kinetic studies, the effect of medium pH on the adsorption capacity of the glutaraldehyde activated (4%, v/v) polyvinylbutyral microbeads was investigated with batch adsorption runs. Figure 6 presents the change of adsorbed BSA at

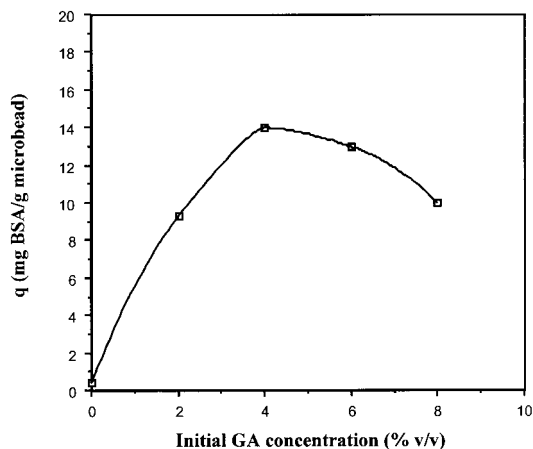


**Figure 5** The change of adsorbed BSA at equilibrium with initial GA concentration (initial BSA concentration 6 mg/mL, pH 7.4, mixing rate 200 rpm,  $25^\circ\text{C}$ ).

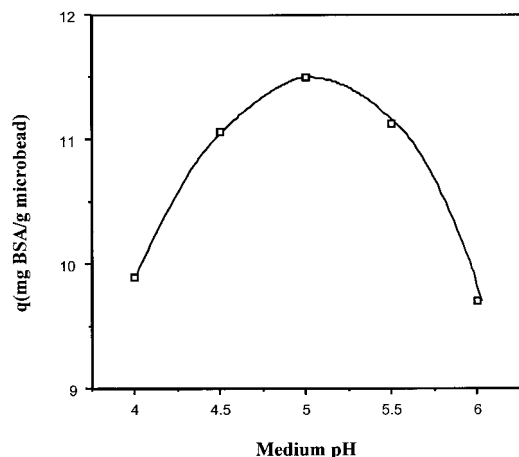


**Figure 6** The variation of adsorbed BSA with medium pH at equilibrium (initial BSA concentration 3 mg/mL, mixing rate 200 rpm, 25°C).

equilibrium as a function of medium pH at different equilibrium BSA concentration values obtained with an initial BSA concentration of 3 mg/mL. The runs were repeated three times, and the average values of corresponding data (with a standard deviation not more than 4%) were presented in the figure. Like other studies in the literature, maximum adsorption of BSA was realized around pH 5,<sup>26</sup> which was the isoelectric point of the protein BSA.<sup>27</sup>

This result is not unusual, because maximum adsorption of a protein can be accomplished when it has a neutral charge, i.e., at the isoelectric point. When neutrally charged, protein solubility in aqueous media decreases. On the other hand, acidic or basic medium caused the protein positively or negatively charged, increasing the solubility of protein in aqueous media. Consequently, lower and higher pH values resulted in decreased adsorption capacities for BSA.

#### The Effect of BSA Concentration on Adsorption Capacity

The amount of BSA adsorbed at optimum pH 5.0 as a function of equilibrium BSA concentration was presented for nonmagnetic and magnetic microbeads in Figure 7. The runs were repeated three times, and the average values of corresponding data (with a standard deviation not more than 4%) were given in the figure.

In the figure, for nonmagnetic microbeads the amount of BSA adsorbed first increased with increasing equilibrium BSA concentration, but reached a plateau value of  $\sim 13$  mg BSA/g mi-

crobead at 4 mg/mL equilibrium BSA concentration. However, for magnetic microbeads adsorption capacity was higher than nonmagnetic ones, being 84 mg BSA/g microbeads at 4 mg/mL equilibrium BSA concentration, and adsorbed amount of BSA continued to increase beyond this concentration. The sigmoid behavior of BSA adsorption for both magnetic and nonmagnetic polyvinylbutyral microbeads is typically represented with a Langmuir type monolayer kinetics. For maximum adsorption capacity of both type of microbeads, the parameter  $q_{\max}$  is obtained from dynamic kinetic model in eq. (2).

#### Desorption of BSA from Microbeads

For assuring the elutability of adsorbed BSA on magnetic and nonmagnetic microbeads (activated with 4% v/v glutaraldehyde), desorption experiments were carried out batchwise at pH 8.0 and 25°C. After 1 h, approximately 91 and 93% of the adsorbed BSA was recovered in the solution from magnetic and nonmagnetic microbeads, respectively.

#### Determination of Adsorption Kinetics

For processing eq. (2) by nonlinear analysis, dynamic data were recorded in batch adsorption runs at several time intervals for magnetic and nonmagnetic microbeads. Time derivative of adsorbed BSA was calculated from the data numerically<sup>25</sup> and presented in Table IIa and b with other variables of eq. (2). The runs were repeated three times, and the average values of corre-

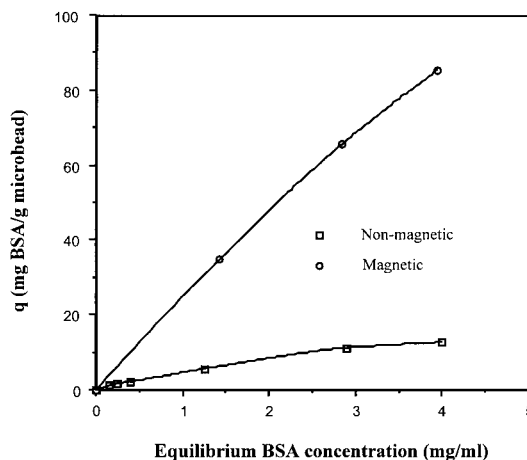


**Figure 7** The change of BSA adsorbed by BSA concentration at equilibrium for magnetic and nonmagnetic microbeads (pH 5.0, mixing rate 200 rpm, 25°C).

**Table II Dynamic Data of BSA Adsorption**

<i>C</i> (mg BSA/mL)	<i>q</i> (mg BSA/g Microbead)	<i>dq/dt</i> (mg BSA/g Microbead/min)
(A) Onto nonmagnetic microbeads		
0	0	0
0.2	1.07	0.004
0.26	1.84	0.07
0.5	2.2	1.1
1.5	5.45	1.82
3.3	11.2	2.24
(B) Onto magnetic microbeads		
0	0	0
1.410	35	8.750
2.840	66	11
3.929	85.45	12

sponding data (with a standard deviation not more than 6%) were given in the tables.

The data in Table IIa and b were processed through Systat®, a nonlinear package program, to yield the best fit of parameters in eq. (2). For nonmagnetic beads,  $q_{\max}$ ,  $k'_f$ , and  $k'_r$  were estimated with a high correlation coefficient ( $r = 0.992$ ) as 17.7 mg BSA/g adsorbent, 0.102 mL/(mg BSA · min) and 0.001 min<sup>-1</sup>, respectively, while the same parameters were found to be 138 mg BSA/g adsorbent, 0.058 mL/(mg BSA · min) and 0.002 min<sup>-1</sup>, respectively ( $r = 0.991$ ), for magnetic microbeads. The maximum BSA adsorption capacity of our magnetic beads is larger than those of other similar works reported in the literature.<sup>2,11-13,28,29</sup> Apparently, magnetic microbeads had a greater adsorption capacity for BSA at equilibrium, however, forward reaction rate,  $k'_f$ , for magnetic microbeads was smaller than that of nonmagnetic microbeads. For both type of microbeads,  $k'_r$  was smaller than  $k'_f$  denoting fast adsorption step. While surface roughness for magnetic microbeads as seen in Figure 3(a) was being an advantage for more binding sites on increased surface area, the same property caused larger liquid film thickness,<sup>30,31</sup> which might have been the reason for low overall forward reaction rate,  $k'_f$ , due to increased mass transfer resistance. Boyer and Hsu investigated the adsorption kinetics for albumin (MW 67000) onto Cibacron Blue attached Sepharose gels using the same kinetic approach.<sup>10</sup> Depending on the concentration of the dye ligand, these workers calculated  $q_{\max}$ ,  $k'_f$ , and  $k'_r$  for albumin in the range

5.26–55.88 mg/cm<sup>3</sup>, 0.085–0.0080 cm<sup>3</sup>/(mg · min), and 0.014–0.0003 min<sup>-1</sup>, having the same order of magnitude of the results obtained in this study. Arnold and Blanch also studied the adsorption of albumin to a lightly substituted reactive blue adsorbent, and the rate constants obtained were of the same magnitude as those found for the work of Boyer and Hsu.<sup>3</sup> Conclusively, our magnetic beads have larger adsorption capacity and comparable forward reaction rates for fast equilibrium, denoting that the microbeads can be a potential protein adsorbent not for only superior separation characteristics but also for high adsorption capacity.

## REFERENCES

- Scopes, R. K. *Protein Purification: Principles and Practice*; Springer-Verlag: Berlin, 1987, 2nd ed.
- Kubota, N.; Kounosu, M.; Saito, K.; Sugita, K.; Watanabe, K.; Sugo, T. *Biotechnol Prog* 1997, 13, 89.
- Arnold, F. H.; Blanch, H. W. *J Chromatogr* 1986, 355, 13.
- Asthan, R.; Polya, G. *Biochem J* 1978, 175, 501.
- Cuatrecasas, P. *J Biochem Chem* 1970, 245, 3059.
- Wilchek, M.; Jakoby, W. B. *Affinity Techniques (Methods in Enzymology)*; Academic Press: New York, 1974, vol. 34.
- Gotoh, M.; Karube, I.; Tamiya, E. *J Mol Catal* 1986, 37, 133.
- Dreyer, W. J.; Rembaum, A.; Yen, S. P. S. *J Cell Biol* 1990, 19, 210.
- Tanyolaç, D. Ph.D. Thesis, Hacettepe University, Ankara, Turkey, 1994.
- Boyer, P. M.; Hsu, J. T. *Chem Eng Sci* 1992, 47, 241.
- Denizli, A.; Salih, B.; Pişkin, E. *J Macromol Sci Pure Appl Chem* 1997, A34, 1352.
- Denizli, A.; Köktürk, G.; Salih, B.; Kozluca, A.; Pişkin, E. *J Appl Polym Sci* 1997, 63, 27.
- Denizli, A.; Salih, B.; Pişkin, E. *J Chromatogr A* 1996, 731, 57.
- Herak, D. C.; Merrill, E. W. *Biotechnol Prog* 1990, 6, 33.
- Denizli, A.; Tanyolaç, D.; Salih, B.; Özduval, A. *J Chromatogr A* 1998, 793, 47.
- Denizli, A.; Tanyolaç, D.; Salih, B.; Aydınlar, E.; Özduval, A.; Pişkin, E. *J Membr Sci* 1997, 137, 1.
- Tanyolaç, D.; Özduval, A. R. *React Funct Polym* 2000, 45, 235.
- Wang, Y. M.; Feng, L. X.; Pan, C. Y. *J Appl Polym Sci* 1998, 70, 2307.
- Ansell, R. J.; Mosbach, K. *Analyst* 1998, 123, 1611.
- Wang, Y. M.; Wang, Y. X.; Feng, L. X. *J Appl Polym Sci* 1997, 64, 1843.



21. Moffat, G.; Williams, R. A.; Webb, C.; Stirling, R. *Minerals Eng* 1994, 7, 1039.
22. Halling, P. J.; Dunhill, M. D. *Enzyme Microb Technol* 1980, 2, 136.
23. Hoechst Mowital® technical data sheet, Section 11, "Polyvinyl butyral resins" in *Synthetic resins for industrial coatings and corrosion protection*, 1984, p. 1.
24. Systat®. Systat Incorporation: Evanston, IL. 1986, version 3.
25. Maron, M. J. *Numerical Analysis: A Practical Approach*; Macmillan Publishing Co. Inc.: New York, 1982, p. 289.
26. Kim, K. S.; Kang, S. H. *Korea Polym J* 1998, 6, 235.
27. Bailey, J. E.; Ollis, D. F. *Biochemical Engineering Fundamentals*; McGraw-Hill Book Company: Singapore, 1986, p. 746, 2nd ed.
28. Denizli, A.; Pişkin, E.; Salih, B. *Turk J Chem* 1995, 19, 296.
29. Denizli, A.; Tuncel, A.; Kozluca, A.; Ecevit, K.; Pişkin, E. *Sep Sci Technol* 1997, 32, 1003.
30. Young, B. D.; van Vliet, B. M. *Int J Heat Mass Transfer* 1988, 31, 27.
31. Dawson, A. D.; Trass, O. *Int J Heat Mass Transfer* 1972, 15, 1317.
32. Arnold, F. H.; Blanch, H. W. *J Chromatogr* 1986, 355, 13.